



PROCESS MONITORING WITH FBG SENSORS DURING VACUUM INFUSION OF THICK COMPOSITE LAMINATES

Patricia P. Parlevliet*, Eli Voet**, Harald E.N. Bersee*, Adriaan Beukers*,***

*Delft University of Technology, Faculty of Aerospace Engineering, Delft, Netherlands

**Ghent University, Department of Mechanical Construction and Production, Ghent, Belgium

***Fellow of Doshisha University, Kyoto, Japan

Keywords: *FBG sensors; vacuum assisted liquid moulding; matrix shrinkage; residual strains*

Abstract

During manufacturing of thick (>20 mm) laminates, thermal gradients through the thickness may arise due to, for example, exothermal reactive heat release. These thermal variations may result in residual strain gradients through the thickness as well as variations in polymer matrix properties, such as degree of cure. For prediction and simulation of the residual strains, it is essential that the manufacturing process is monitored, in order to identify the parameters responsible for the residual strain build-up.

The research described in this paper, proposes the use of Fibre Bragg Grating sensors as an experimental tool to determine variations in (thermal) residual strain levels through the thickness in a thick glass fibre reinforced thermoset laminate. In addition, other manufacturing issues, such as the flow behaviour that could be identified with these sensors were addressed. Moreover, the results of a first attempt to identify polymer property variations through the thickness by means of the microhardness test are reported.

1 Introduction

Thick composite laminates are increasingly applied in high-performance structures, such as wind turbine blades, pressure vessels, parts in aircrafts, bridges, etc. These structures can be manufactured with filament winding, vacuum infusion, and hand lay-up. Currently, thick (>20mm) laminates are mostly prepared of thermoset matrix composites by means of the liquid moulding technology.

During processing, through-the-thickness gradients may arise in, for example, temperature or degree of cure. This may lead to a residual strain distribution within the part as well as a gradient in material properties [1]. For engineering purposes, it

is desired that the composite structure shows homogeneous properties over the entire structure. In order to predict the residual strains, it is essential that the behaviour of the polymer matrix composite during processing is known. Several parameters can be of influence to the residual strain build-up of a fibre reinforced polymer laminate [2]. In this case, the temperature difference between the strain free temperature (the temperature from which strains start building up) and the service temperature (often room temperature), in combination with the shrinkage of the laminate between these temperatures, are of most importance [3]. Here, we assume that the strain free temperature corresponds to the peak temperature that develops due to the exothermal reaction. Therefore, if a variation in peak temperature exists through the thickness of a composite laminate, this will result in a residual strain variation through the thickness. One promising experimental technique to investigate these residual strain variations is the use of optical fibre sensors, such as Fibre Bragg Gratings. Therefore, this paper describes investigations into how optical fibres with Bragg gratings can be utilised to study the behaviour of the pure polymer matrix as well as glass fabric reinforced laminates during processing.

This study will investigate process properties of thick laminates manufactured with vacuum infusion of a thermoset matrix: a commercially available room-temperature curing hybrid polyurethane/ polyester. The hybrid Daron® resin system is a low viscosity, room temperature curing system with a short processing cycle (total cycle time ~90 minutes). It shows a very high generation of exothermal heat, due to which a high peak temperature is reached. This peak temperature determines the glass transition temperature or heat

deflection temperature. One experimental technique that can be used to assess the glass transition temperature (T_g) (and hence the degree of conversion, since the two parameters are related), is the microVickers indentation test (microhardness). Microhardness testing is an easy and useful tool to determine property variations of the matrix in a composite with, because it can test the matrix in between the fibre bundles [4]. As said earlier, the peak temperatures determine the T_g of the polymer matrix. The further the temperature below the T_g of the polymer is, the harder the polymer. Therefore, this technique is used to identify a trend in T_g variations.

2 Theoretical Background

Recent developments show that fibre optical sensors (FOSs) can be applied as internal “strain gauges” to follow the development of thermal residual strains inside a composite laminate, even during processing at the high temperatures needed for thermoplastic composites [5, 6]. The FBG sensors are regarded as very promising for monitoring residual strain development during processing [5, 7-12], due to their small diameter and accuracy. Applications were found in unidirectional laminates as well as in angle-ply laminates.

The working principle of an optical fibre sensor with a single axial Bragg grating (single mode optical fibre) is illustrated in Fig. 1.

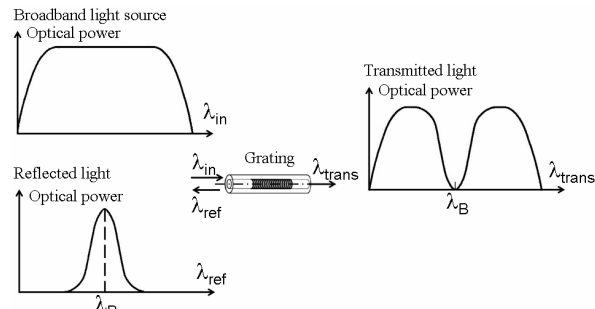


Fig. 1. Working principle of an optical fibre Bragg grating (FBG) [13].

Broadband light is transmitted through the single mode optical fibre. Bragg gratings are located at certain points in this optical fibre, which act as wavelength selective mirrors. For each grating only one wavelength, the Bragg wavelength λ_B , is reflected, while all other wavelengths are transmitted. As a result, information can be acquired

from both ends of the fibre. A detailed image of such grating is given in Fig. 2.

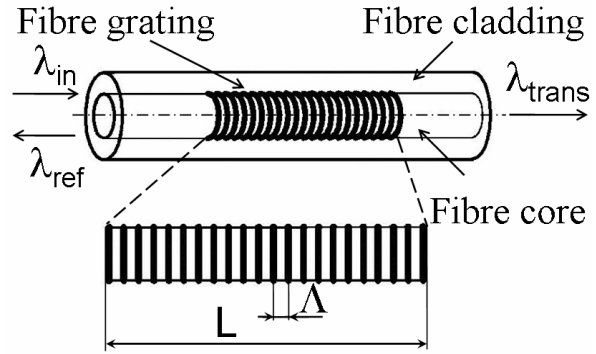


Fig. 2. Bragg grating detail [13].

A fibre Bragg grating is actually no more than an area in the core of the fibre with successive zones with alternating refractive index. If Δ is the period or spacing of the grating, then the Bragg wavelength of the grating is given by [14]:

$$\lambda_B = 2n_{eff} \Delta \quad (1)$$

where n_{eff} is an averaged refractive index over the length L of the grating. Consequently, the length L changes if a strain is imposed on the optical fibre. As such, a measurement of the strain is achieved: the difference between the wavelength of the strained and the unstrained grating increases linearly with the imposed strain [14]. The difference in wavelength $\Delta\lambda$ can be related to the strain and temperature behaviour of the fibre Bragg grating, with the following linear approximation [15]:

$$\Delta\lambda = s_\epsilon \Delta\epsilon + s_T \Delta T \quad (2)$$

Typical values for the constants s_ϵ and s_T for an FBG in the typical wavelength band region (1520nm – 1560nm) are 1.2 pm/ $\mu\epsilon$ and 10 pm/ $^\circ\text{C}$ respectively [15]. It should be noted that these sensitivities are in fact wavelength dependent – they are directly proportional to the FBG-wavelength λ_B - but for small wavelength changes they are normally approximated as being constant. If the wavelength shifts are in the order of a few nanometres, the relative error induced by using the (linear) sensitivities to calculate the strain or temperature are small and are kept below 1%.

As is clear from Eq. 2, an FBG is sensitive to both strain and temperature. This actually means that always two FBG's are needed, one to measure strain and one to measure temperature. This latter is necessary to compensate for wavelength shifts due

to temperature fluctuations. Therefore, for determination of the developing strains during manufacturing, for example during the reaction, it is essential that the wavelength shifts due to the thermal variations is recorded correctly. This means that the temperature sensors (the FBG inside the capillary), must be free from any strains imposed by the surrounding laminate. A relatively easy method to achieve this is to use a capillary or a ferrule design, where the second FBG is kept strain-free, see also Fig 3. This can be validated by checking whether the wavelength as indicated by the temperature FBG, is equal at similar temperatures. If this is not the case, the temperature FBG readings must be disregarded.

In essence, it must be possible to distinguish between the curing shrinkage effect of the polymer matrix and the cooling shrinkage by means of the FBG sensors when a wavelength versus temperature graph can be obtained [8, 9, 18]. Moreover, the combination of a FBG sensor utilised as a temperature sensor and a FBG strain sensor, renders it possible to determine the CTE upon cooling of the matrix and laminate [16].

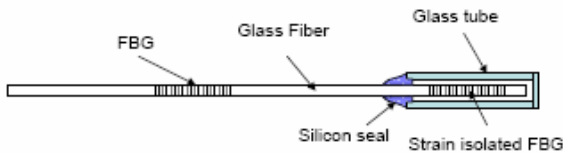


Fig. 3. Schematic view of a FBG based temperature sensor [16].

An important advantage of FBG sensors is that more than one FBG can be located in one optical glass fibre, due to which more sensing points can be read out at the same time. This makes it possible to have more measurements per layer of the laminate, of which average values and standard deviations can be calculated to improve the accuracy of the experiment. In addition, multiple gratings per optic fibre makes it possible to monitor flow behaviour of the liquid resin through the vacuum bagged reinforcement, provided the FBG sensors show the passing of the flow front. This is investigated in this research as well.

3 Experimental Techniques

3.1 Materials

1 kg of Daron® ZW6154 hybrid system (DSM Composite Resins, Netherlands) was mixed with 20 g of peroxide (Lucidol® CH50X, Akzo Nobel,

Netherlands) to form component A. 350 g of Lupranate® M20R (DSM Composite Resins) was mixed with 20 g Accelerator (NL64-10P, Akzo Nobel) to form component B. After mixing the two components, the liquid was degassed for 5 minutes in a vacuum oven. As reinforcement, 21 layers of 20 x 20 cm non-crimp fabric with flow mat were used (Unifilo® 1300-935-450, Saint Gobain Vetrotex).

3.2 Specimen Preparation

For identification of the polymerisation behaviour of the pure matrix, a glass cylinder was used in which a thermocouple and an optical fibre with three FBG sensors were placed in the centre, of which two were surrounded by a capillary for the grating to function as a temperature sensor. The reactive mixture was poured inside the glass cylinder after which reaction could take place. The thermocouple was used to record only the peak temperature.

For the thick laminate, a 1.5 mm thick aluminium plate was coated with release agent (Waterworks Departure®) and the reinforcement plies were stacked. The fibre optic sensors were placed according to the lay-out in Fig. 4. The dotted sensor parts depict the strain sensors and the orange parts represent the temperature sensors. This system was then vacuum bagged. Vacuum pressure during infusion was 20 mbar and after infusion the pressure was decreased to 500 mbar. This resulted in a laminate of 34 mm thickness. A similar laminate was made in which thermocouples instead of optic fibres were placed to monitor the exothermal temperature profile.

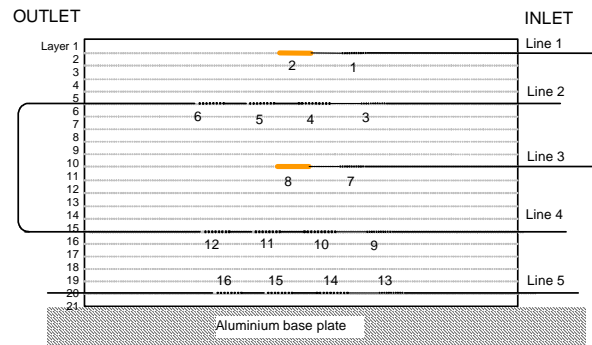


Fig. 4. Schematic lay-out of the FBG sensors placed in the laminate cross section

3.3 Test set-up

3.3.1 Fibre Bragg Grating sensors

The fibre optic sensors used for these embedding experiments are Draw Tower fibre Bragg gratings (DTG[®]'s), provided by FBGS-Technologies GmbH, Jena (Germany). Such gratings are manufactured during the fabrication process of the optical fibre and are coated immediately after the inscription of the Bragg grating [17]. The optical fibres with an Ormocer[®] coating (cladding diameter 125 μm) were supplied by FOS&S, Geel, Belgium. For the temperature sensors, the gratings were surrounded by flexible fused silica tubing, which was coated with a polyimide layer.

In order to calculate residual strains from the wavelengths, one has to take the difference in wavelength and divide that by a constant that relates this change in wavelength to strain levels, see Eq. 2, provided the temperature is equal ($\Delta T = 0$). For the optical sensors used here, this constant s_e is 1.21 pm/ μstrain . Residual strains were determined by taking the wavelength directly after infusion (the optic fibre is assumed to be in a relaxed state) and compare them to the wavelengths as measured at the end of the day when the laminate was cooled to 28°C and only a small temperature gradient through the thickness remained (1.2°C difference between the surface and the centre respectively). Resin temperature during infusion was 24°C, so there still is a small difference in wavelength due to the temperature difference of 4°C (the gratings expand on increasing temperature, hence giving a higher wavelength), but this is expected not to affect the values of the calculated residual strains significantly.

In addition, it was determined if the strains generated by the shrinkage of the matrix were transferred to the optical fibre correctly. This was done by comparing the shrinkage behaviour as measured by the FBG sensors with the shrinkage as determined with a gravimetric method.

Moreover, the readings from the FBGs were used to identify the flow behaviour of resin inside the laminate.

3.3.2 Temperature

Besides the use of FBG temperature sensors, K-type thermocouples were placed between similar layers as the fibre optic sensors were placed. Their readings were recorded with a Keithley data logging device. This was done for a second laminate, manufactured in exactly the same fashion.

3.3.3 Polymer properties

On a similar laminate manufactured on a glass base plate (to obtain a symmetrical thermal profile through the thickness due to two thermal insulating sides; the vacuum bag side and the glass side), the variation in microhardness through the thickness was tested. Temperature recordings were taken in this laminate also, as described in Section 3.3.2. A Buehler Omnimet[®] MHT hardness tester was used with a 25 gram load. The load was applied for 15 seconds and the test environment consisted of ambient conditions (room temperature $\sim 21^\circ\text{C}$ and relative humidity $\sim 70\%$). The lengths of the diagonals were determined utilising a CCD camera in combination with the Omnimet[®] software program on a Windows 2000 based personal computer. The hardness values were calculated using Eq. 3 and multiplied with the gravitational constant (9.81) to obtain the values in MPa units.

$$HV = 2 \sin\left(\frac{136}{2}\right) \frac{F}{d_1 \cdot d_2} \quad (3)$$

where F is the load in kgf and d_1 and d_2 are the lengths of the diagonals in mm . The Vickers hardness is usually reported as $800\text{ HV}10$, which means a Vickers hardness of 800 was obtained using a 10 kgf force. The term microhardness usually refers to static indentations made with loads lower than 1 kgf [19, 20]. Five distinct plies were chosen, similar to those where the thermocouples were placed, and along every ply a minimum of 10 indentations were made. This resulted in average hardness values with a standard deviation for these plies.

3.4 Prediction of thermal residual strains

The thermal residual strains as detected by the FBG sensors can be predicted by taking the temperature difference between the peak temperature and the end temperature (ΔT) and multiply that with the difference in coefficient in thermal expansion (CTE) between the laminate α_c and the optical fibre α_{FBG} :

$$\varepsilon = (\alpha_c - \alpha_{\text{FBG}}) * \Delta T \quad (4)$$

The CTE of the composite is calculated with rules-of-mixture [21] and the material property values as given by Ref [22], which results in a value of $9.4 * 10^{-6} \text{ K}^{-1}$, and for the FBG sensor the CTE is given as $0.55 * 10^{-6} \text{ K}^{-1}$ [23].

4 Results

4.1 Polymerisation of the pure polymer matrix

The wavelength versus time graphs for the determination of the polymer shrinkage during curing is given in Fig. 5.

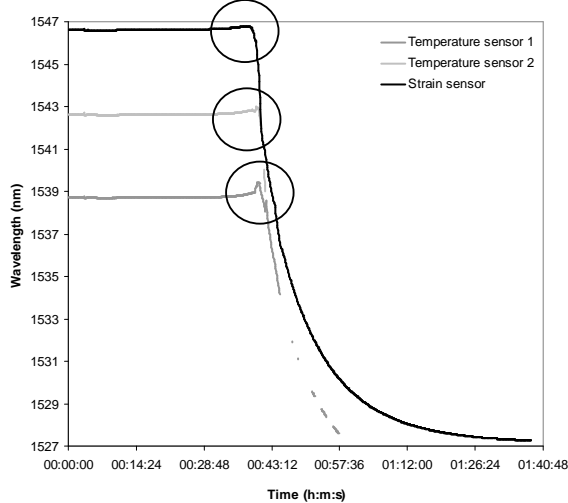


Fig. 5. Wavelength changes due to polymerisation of pure matrix.

The temperature sensors as well as the strain sensors give a good indication of when the polymerisation reaction starts for this matrix, as indicated by the shift in wavelength to higher values after approx. 36 minutes. The peak temperature reading was 135°C. However, only the strain sensor was capable of following the entire shrinkage of the polymer matrix, whereas the temperature sensors failed during the process. This may be attributed to a loss of signal power, since no peak splitting was observed. Peak splitting occurs when birefringence occurs in the optical fibre (instead of circular, the cross-section becomes elliptically in shape, resulting in two wavelength peaks).

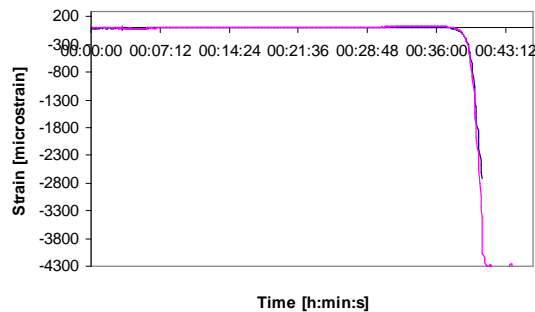


Fig. 6. Development of curing strain as determined with a FBG sensor

When subtracting the temperature wavelength readings (for the values that we were able to determine) from the strain wavelength readings, and correcting for the strain constant s_e with Eq. 2, Fig. 6 is obtained. This figure clearly shows that the strain can be monitored without the effects of the temperature variations due to the exothermal reaction, which are still clearly present in the wavelength graphs (indicated by the circles). This allows us to identify the time to start of the curing shrinkage. Curing shrinkage starts at ~36.26 min, and the peak temperature is reached at ~40.17 min. Before and after curing (at room temperature, $\Delta T = 0$, the wavelength difference of the strain sensor is 19.495 nm, which corresponds to a residual strain of 1.6%. In comparison to the values given by the manufacturer and as checked with a gravimetric analysis tool [24] (both gave ~6% shrinkage), this value is rather low. More research is necessary to find out the causes for this discrepancy. One explanation can be that the strain transfer was not optimal due to poor adhesion between the optical fibre and the matrix.

In addition, the temperature sensors show compressive strain build-up (the wavelength is lower after curing of the polymer), which indicates that they have not been free from strain. When comparing the peak temperature as indicated by the thermocouple (135°C) and the temperature as indicated by the wavelength shift (calculated as follows: at 24°C before infusion $\lambda = 1538.721$ nm, at the peak temperature $\lambda = 1539.434$ nm, giving $\Delta\lambda = 0.713$ nm, with Eq. 2 and $s_T = 12.2$ pm/°C) results in a peak temperature of 82°C, which is far from the actual peak temperature. Clearly more research is necessary to solve this.

4.2 Thick laminate

In Table 1, the important wavelengths are given, as well as the residual strain calculation per grating. The orange numbers represent the values as determined with the temperature FBGs.

Regarding the temperature sensors, again a compressive strain was found even higher than their accompanying strain sensor, rendering it impossible to determine the strain build-up during manufacturing.

Table 1. Comparison of wavelengths before and after curing and the calculated resulting strain.

		λ_1 [nm]	λ_2 [nm]	$\Delta\lambda = \lambda_1 - \lambda_2$ [nm]	Strain [%]
Line 1	1	1537.382	1536.59	-0.792	-0.065
	2	1530.222	1529.163	-1.059	-0.088
Line 2	3	1531.863	1530.903	-0.960	-0.079
	4	1534.777	1533.918	-0.859	-0.071
	5	1537.896	1537.004	-0.892	-0.074
	6	1540.835	1539.701	-1.134	-0.094
Line 3	7	1557.605	1556.777	-0.828	-0.068
	8	1563.448	1562.516	-0.932	-0.077
Line 4	9	1543.914	1543.130	-0.784	-0.065
	10	1546.688	1546.034	-0.654	-0.054
	11	1549.702	1548.58	-1.122	-0.093
	12	1552.992	1552.036	-0.956	-0.079
Line 5	13	1544.136	1543.554	-0.582	-0.048
	14	1546.837	1546.461	-0.376	-0.031
	15	1550.177	1549.603	-0.574	-0.047
	16	1553.113	1552.363	-0.750	-0.062
Pure resin		1546.621	1527.28	-19.341	-1.60

Table 2. Temperature and strain values

	Peak T [°C]	End T [°C]	Calculated strain [%]	Experimental strain (FBG) [%]
Line 1	118.4	28.4	-0.080	-0.065
Line 2	130.4	28.6	-0.090	-0.075 ± 0.004
Line 3	128.6	28.5	-0.089	-0.068
Line 4	115.1	28.1	-0.077	-0.073 ± 0.017
Line 5	75.0	27.4	-0.042	-0.042 ± 0.010

First of all, it is clear that a temperature profile exists through the thickness as a result of the exothermic heat release and the poor thermal conductivity of the composite material. In other words, the heat generated in the thermal centre cannot easily dissipate away and a temperature rise is the result. It may be noted that the aluminium base plate (on the right hand side of the graph/laminate) acts as a heat sink, due to which the peak temperatures are lower on that side and the temperature profile is not symmetrical. The yellow point is the peak temperature as measured on the outside of the vacuum bag.

The peak temperatures, experimentally measured residual strains as well as the calculated residual strains (Eq. 4) of the 34 mm laminates are given in Fig. 7. Their corresponding data are given in Table 2. Please note that the strains are depicted in a positive manner for clarity purposes, but they are compressive in nature. Please note that for layer 1 and 11 only one strain measurement was available.

As is clear from Fig. 7, the variation in peak temperature is reflected in the variation of the residual strains. Therefore, it may be concluded that the variation in peak temperature indeed does lead to a variation in residual strain through the thickness of a thermoset laminate. However, the calculated strains overestimate the experimentally obtained residual strains, except for the lower strain values. Further research is required to understand this.

4.3 Microstructure

The results of the microhardness test and the corresponding peak temperatures are shown in Fig. 8. Please note that these tests were done on a similar laminate as discussed previously, but now manufactured on a glass base plate, resulting in a different (almost symmetrical) temperature profile.

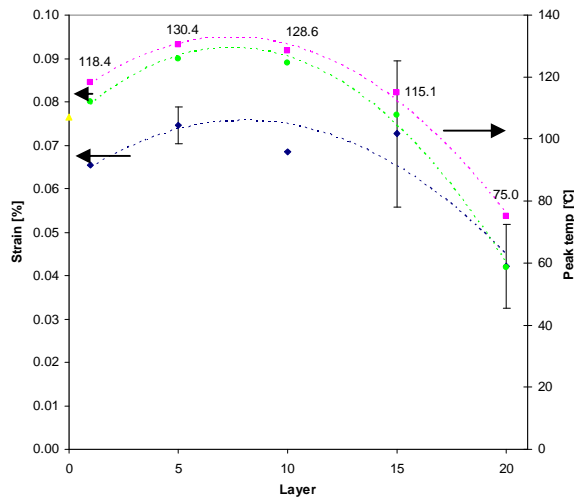


Fig. 7. Variation of peak temperature (pink data) and residual compressive strains (experimental: blue data, calculated: green data) through the thickness

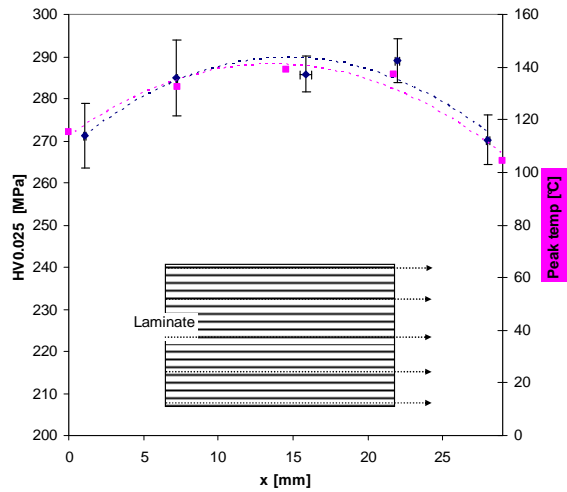


Fig. 8. Microhardness and peak temperatures

Again, similar trends can be observed between the peak temperatures and microhardness. This means that a variation in peak temperature induces a variation in polymer properties through the thickness. For confirmation of the relation between T_g and microhardness, as described in Section 1, determination of T_g variations through the thickness by means of differential scanning calorimetry (DSC) can be carried out, but at the moment of writing this paper, the results were not yet available.

4.4 Flow behaviour

As indicated by the arrow in Fig. 9, when the resin flow front passes an FBG, this is immediately reflected in a sudden wavelength shift. This allows us to monitor the filling of the reinforcement or mould.

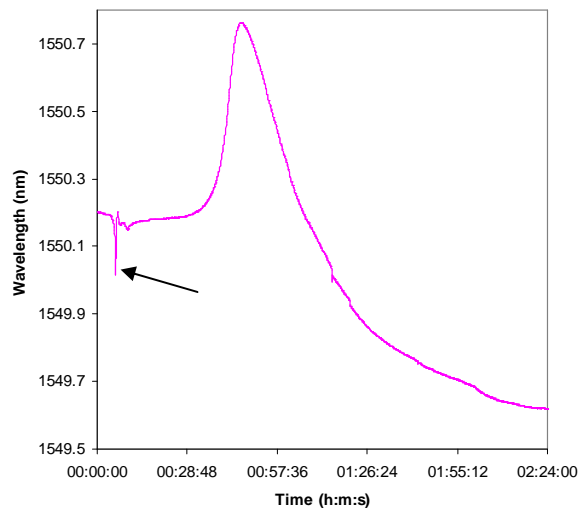


Fig. 9. Wavelength versus time (FBG nr 15)

In Table 3 and Figure 10, the times and a schematic view of the resin flow behaviour are given, respectively. The black dots in Fig. 10 indicate the FBGs. The flow front clearly prefers the smooth mould side (bottom of the picture).

Table 3. Time of passing flowfront

	Time [min.s]
Line 1	1 5.27
	2 6.20
Line 2	3 5.01
	4 5.48
	5 6.51
Line 3	6 7.39
	7 5.52
	8 6.21
Line 4	9 4.56
	10 5.25
	11 6.22
	12 7.20
Line 5	13 4.52
	14 5.11
	15 5.55
	16 6.57

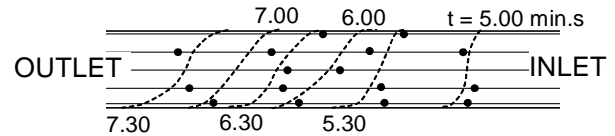


Fig. 10. Schematic view of resin flow behaviour

5 Discussion and Conclusions

A 3 cm thick glass reinforced hybrid polyurethane/ polyester laminate was manufactured, of which the temperatures during the reaction were measured. The temperature readings clearly indicate a thermal gradient through the thickness. The measured variation in peak temperatures can be related to the thermal residual strain levels as well as the polymer properties, in this case the glass transition temperature, through the thickness after manufacturing. Residual strains were identified by means of the fibre Bragg gratings and the polymer matrix properties by means of microhardness tests. The residual strain gradient seems to originate mainly from the thermal shrinkage of the laminate when cooling down to the service temperature from the varying peak temperatures, although the FBGs showed a lower strain than the calculated one. In addition, the FBG sensors showed to be useful to monitor the flow behaviour inside a thick laminate.

Pressure differences due to the passing of this flow front were clearly indicated by the sensors.

The temperature sensors as used for this research did not fulfil the requirement of being protected from external strain sources. Therefore, the readings of these sensors could not be used to subtract the wavelength shifts due to temperature variations from the strain sensor readings. Due to this, we were unable to construct a wavelength versus temperature graph as explained in Section 3.3.1. Therefore it is impossible to fully identify the governing process parameters for residual strain build-up. In effect, it should be possible to reconstruct the wavelength shifts due to temperature variations by means of temperature readings and the thermal coefficient (Eq. 2). However, temperature readings were carried out on a different laminate, and when trying this, the results were not very accurate. Therefore, this is not included in this paper.

Note from the authors

This work is part of a project titled ‘Microstructure and Residual Strains in Thick Thermoplastic laminates’. The final goal of this project is to understand the relations between the triangle ‘processing – microstructure – properties’ when manufacturing a thick fibre reinforced thermoplastic composite laminate. Researchers at Delft University of Technology have developed a new technology including a thermoplastic matrix material and the vacuum infusion technique for manufacturing thick-walled structures with a thermoplastic matrix. This matrix is the anionically polymerising polyamide-6 (APA-6) system [25]. Advantages are: shorter processing cycles (1 hour), assembly by welding is possible and the matrix can be recycled into the initial components. Preliminary studies showed that thick laminates of good quality can be produced with these matrices [26]. However, since this system is still under development, and the FBGs are still rather expensive, we chose to test the experimental technique of FBG sensors on a proven matrix system, with a similar processing technology as required for the APA-6 laminates. Preliminary results for FBG sensors in combination with the APA-6 system and thin laminates can be found in the accompanying abstract. However, for this full-length paper, the authors chose to explain the tests and results as obtained with the thick “proven technology” laminate.

Acknowledgements

The authors would like to thank FOS&S, Geel, Belgium and Jasper Bouwmeester, DSM Composite Resins, Zwolle, Netherlands, for their support.

References

- [1] Parlevliet, P.P., H.E.N. Bersee, and A. Beukers, *Residual Stresses in Thermoplastic Composites - A Study of the Literature - Part III: Effects of Thermal Residual Stresses*. Composites Part A: Applied Science and Manufacturing. **38**(6): p. 1581-1596, 2007.
- [2] Parlevliet, P.P., H.E.N. Bersee, and A. Beukers, *Residual Stresses in Thermoplastic Composites - A Study of the Literature - Part I: Formation of Residual Stresses*. Composites Part A-Applied Science and Manufacturing. **37**(11): p. 1847-1857, 2006.
- [3] Li, C., et al., *In-situ measurement of chemical shrinkage of MY750 epoxy resin by a novel gravimetric method*. Composites Science and Technology. **64**(1): p. 55-64, 2004.
- [4] van der Werf, A.W., *MicroVickers indentation as an analysis tool for matrix properties in thermoplastic composites*, in *Aerospace Engineering*. Delft University of Technology: Delft. 2006
- [5] Sorensen, L., T. Gmür, and J. Botsis. *Residual Strain Development in Laminated Thermoplastic Composites Measured Using Fibre Bragg Grating Sensors*. in *Proceedings of CompTest 2004*. Bristol, UK. 2004.
- [6] Vlekken, J., *Fibre Bragg Grating sensors for monitoring thermoplastic composite processing*. Personal communication. 2004.
- [7] Okabe, Y., et al., *Detection of transverse cracks in CFRP composites using embedded fiber Bragg grating sensors*. *Smart Materials & Structures*. **9**(6): p. 832-838, 2000.
- [8] O'Dwyer, M.J., et al., *Relating the state of cure to the real-time internal strain development in a curing composite using in-fibre Bragg gratings and dielectric sensors*. *Measurement Science and Technology*. **9**(8): p. 1153-1158, 1998.
- [9] Chehura, E., et al., *Strain development in curing epoxy resin and glass fibre/epoxy composites monitored by fibre Bragg grating sensors in birefringent optical fibre*. *Smart Materials & Structures*, **14**(2): p. 354-362, 2005.
- [10] Kuang, K.S.C., et al., *Process monitoring of aluminum-foam sandwich structures based on thermoplastic fibre-metal laminates using fibre*

- Bragg gratings*. Composites Science and Technology, **65**(3-4): p. 669-676, 2005.
- [11] Okabe, Y., et al., *Effect of thermal residual stress on the reflection spectrum from fiber Bragg grating sensors embedded in CFRP laminates*. Composites Part a-Applied Science and Manufacturing, **33**(7): p. 991-999. 2002.
- [12] Okabe, Y., et al., *Detection of microscopic damages in composite laminates with embedded small-diameter fiber Bragg grating sensors*. Composites Science and Technology, **62**(7-8): p. 951-958, 2002.
- [13] De Waele, W., *Structural monitoring of composite elements using optical fibres with Bragg-sensors*. Ghent University. 2002
- [14] Grattan, K.T.V. and B.T. Meggitt, *Optical fibre sensor technology: Fundamentals*, Dordrecht: Kluwer academic publishers, 2000.
- [15] Luyckx, G., et al., *Three-dimensional strain and temperature monitoring of composite laminates*. Insight, **49**(1): p. 10-16. 2007.
- [16] Fernandez-Lopez, A., A. Guemes, and J.M. Menendez. *Measuring the thermal expansion coefficient of composite laminates by fiber optic sensors*. in SAMPE Europe International Conference 2007. Paris. 2007.
- [17] Chojetzki, C., et al., *Large Fibre Bragg Grating Arrays for monitoring applications - Made by Drawing Tower Inscription*. IPHT & FOS&S: Jena, Germany & Geel, Belgium. 2005
- [18] Antonucci, V., et al., *Real time monitoring of cure and gelification of a thermoset matrix*. Composites Science and Technology, **66**(16): p. 3273-3280. 2006.
- [19] ASTM International, *ASTM E384-05a: Standard Test Method for Microindentation Hardness of Materials*. 2005. p. 24.
- [20] England, G., *Hardness testing*, <http://gordonengland.co.uk/hardness/microhardness.htm>.
- [21] Cowley, K.D. and P.W.R. Beaumont, *The measurement and prediction of residual stresses in carbon-fibre/polymer composites*. Composites Science and Technology, **57**(11): p. 1445-1455. 1997.
- [22] Andersson, B., A. Sjogren, and L. Berglund, *Micro- and meso-level residual stresses in glass-fiber/vinyl-ester composites*. Composites Science and Technology, **60**(10): p. 2011-2028. 2000.
- [23] Hagemann, V.J., *Untersuchungen zum dynamischen Einzelpuls-Einschreiben von Faser-Bragg-Gittern und zu deren Anwendung*. 2001.
- [24] Veloso Navarro, R., *Development of a Test Setup for measuring of Chemical Shrinkage in Polymers*. Delft University of Technology: Delft. 2006
- [25] van Rijswijk, K., *Thermoplastic Composite Wind Turbine Blades*, in *Aerospace Engineering*. Delft University of Technology: Delft. p. 249. 2007.
- [26] Baten, E.M., *Microstructural Variations in Thick-Walled Anionic Polyamide-6 Composites*, in *Aerospace Engineering*. Delft University of Technology: Delft. p. 80. 2006.